EPJ Web of Conferences **291**, 05011 (2024) https://doi.org/10.1051/epjconf/202429105011
MESON 2023

Measurement of $\bar{K}N$ scattering below the $\bar{K}N$ mass threshold

Hiroyuki Noumi[1,20,*], *Kentaro* Inoue[1,**], *Shingo* Kawasaki[1,***], *Shuu* Aikawa[2], *Shuhei* Ajimura[1], *Takaya* Akaishi[3], *Hidemitsu* Asano[4], *George* Beer[5], *Carolina* Berucci[6], *Mario* Bragadireau[7], *Paul Alois* Buehler[6], *Luigi* Busso[8,9], *Michael* Cargnelli[6], *Seonho* Choi[10], *Catalina* Curceanu[11], *Shun* Enomoto[12], *Hiroyuki* Fujioka[2], *Yuya* Fujiwara[13], *Tomokazu* Fukuda[14,15], *Carlo* Guaraldo[11], *Tadashi* Hashimoto[16], *Ryugo S.* Hayano[13], *Toshihiko* Hiraiwa[17], *Masami* Iio[18], *Mihai* Iliescu[11], *Yusuke* Ishiguro[19], *Shigeru* Ishimoto[20], *Takashi* Ishikawa[13], *Kenta* Ithashi[4], *Massaki* Iwai[21], *Masahiko* Iwasaki[4,2], *Koki* Kanno[13], *Kazuma* Kato[14], *Yuko* kato[4], *Paul* Kienle[22], *Yusuke* Komatsu[20], *Hiroshi* Kou[2], *Yue* Ma[4], *Johann* Marton[6], *Yasuyuki* Matsuda[23], *Yutaka* MIzoi[14], *Ombretta* Morra[8], *Rie* Murayama[4], *Tomofumi* Nagae[14], *Hiroaki* Ohnishi[24], *Shinji* Okada[4], *Zhadyra* Omar[1,25], *Haruhiko* Outa[4], *Kristian* Piscicchia[26,27], *Yuta* Sada[24], *Atsushi* Sakaguchi[3], *Fuminori* Sakuma[4], *Masaharu* Sato[12], *Alessadro* Scordo[11], *Michiko* Sekimoto[20], *Hexi* Shi[11], *Kotaro* Shirotori[1], *Diana* Sirghi[11,7], *Florin* Sirghi[11,7], *Ken* Suzuki[6], *Shoji* Suzuki[20], *Takatoshi* Suzuki[13], *Kiyoshi* Tanida[16], *Hideyuki* Tatsuno[28], *Atsushi O.* Tokiyasu[24], *Makoto* Tokuda[2], *Dai* Tomono[1], *Akihisa* Toyoda[20], *Kyo* Tsukada[4], *Oton* Vazquez-Doce[11,29], *Eberhard* Widmann[6], *Takumi* Yamaga[4], *Toshimitsu* Yamazaki[13], *Heejoong* Yim[30], *Qi* Zhang[4], and *Johannes* Zmeskal[6] [J-PARC E31 collaboration]

[1]Research Center for Nuclear Physics, Osaka University, Ibaraki, 567-0047, Japan
[2]Department of Physics, Tokyo Institute of Technology, Tokyo, 152-0551, Japan
[3]Department of Physics, Osaka University,Toyonaka, 560-0043, Japan
[4]RIKEN Cluster for Pioneering Research (CPR), RIKEN, Wako, 351-0198, Japan
[5]Department of Physics and Astronomy, University of Victoria, Victoria BC V8W 3P6, Canada
[6]Stefan-Meyer-Institut für subatomare Physik, A-1030 Vienna, Austria
[7]National Institute of Physics and Nuclear Engineering (IFIN-HH), Magurele, Romania
[8]INFN Sezione di Torino, Torino, Italy
[9]Dipartimento di Fisica Generale, Universita'di Torino, Torino, Italy
[10]Department of Physics, Seoul National University, Seoul, 151-742, South Korea
[11]Laboratori Nazionali di Frascati dell'INFN, I-00044 Frascati, Italy
[12]Accelerator Laboratory, High Energy Accelerator Research Organization (KEK), Tsukuba, 305-0801, Japan
[13]Department of Physics, The University of Tokyo, Tokyo, 113-0033, Japan
[14]Laboratory of Physics, Osaka Electro-Communication University, Neyagawa, 572-8530, Japan
[15]RIKEN Nishina Center for Accelerator-Based Science, RIKEN, Wako, 351-0198, Japan
[16]ASRC, Japan Atomic Energy Agency (JAEA), Ibaraki 319-1195, Japan
[17]RIKEN SPring-8 Center, RIKEN, Hyogo, 679-5148, Japan
[18]Cryogenics Science Center, High Energy Accelerator Research Organization (KEK), Tsukuba, 305-0801, Japan
[19]Department of Physics, Kyoto University, Kyoto, 606-8502, Japan

[*]e-mail: noumi@rcnp.osaka-u.ac..jp
[**]e-mail: kentaro@rcnp.osaka-u.ac.jp
[***]e-mail: shinngo@rcnp.osaka-u.ac.jp

[20]Institute of Particle and Nuclear Studies, High Energy Accelerator Research Organization (KEK), Tsukuba, 305-0801, Japan
[21]Mechanical Engineering Center, High Energy Accelerator Research Organization (KEK), Tsukuba, 305-0801, Japan
[22]Technische Universität München, D-85748, Garching, Germany
[23]Graduate School of Arts and Sciences, The Univeristy of Tokyo, Tokyo, 153-8902, Japan
[24]Research Center for Electron Photon Science (ELPH), Tohoku University, Sendai, 982-0826, Japan
[25]Department of Physics, Al-Farabi Kazakh National University, Almaty, 050040, Kazakhstan
[26]Museo Storico della Fisica e Centro Studi e Ricerche "Enrico Fermi", Piazza del Viminale 1, 00184 Rome, Italy
[27]INFN, Laboratori Nazionali di Frascati, Via Enrico Fermi 40, 00044 Frascati, Italy
[28]Department of Chemical Physics, Lund University, Lund, 221 00, Sweden
[29]Excellence Cluster University, Technische Universität München, D-85748, Garching, Germany
[30]Korea Unstitute of Radiological and Medical Sciences (KIRAMS), Seoul, 139-706, South Korea

Abstract. We measured $\pi\Sigma$ invariant mass spectra below and above the $\bar{K}N$ mass threshold in the $K^-d \to N\pi\Sigma$ reaction in order to study the $\bar{K}N$ interaction and the $\Lambda(1405)$ resonance. This reaction can be described by the two-step process: (i) $K^-N_1 \to \bar{K}N$ followed by (ii) $\bar{K}N_2 \to \pi\Sigma$, where N_1 and N_2 are nucleons bound in the deuteron. We deduced the S-wave scattering amplitude of $\bar{K}N \to \bar{K}N$ as well as $\bar{K}N \to \pi\Sigma$ in $I = 0$ in the framework of the $\bar{K}N$-$\pi\Sigma$ coupled channel so as to reproduce the observed $\pi\Sigma$ spectra in the $I = 0$ channel. We found a resonance pole at $1417.7^{+6.0}_{-7.4}$(fitting error)$^{+1.1}_{-1.0}$(systematic error)$-i[26.9^{+6.0}_{-7.9}$(fitting error)$^{+1.7}_{-2.0}$(systematic error)] MeV/c^2.

1 Introduction

$\Lambda(1405)$ is a well-established hyperon resonance with the spin/parity of $1/2^-$. However, internal structure of $\Lambda(1405)$ is still unclear. In the constituent quark model, $\Lambda(1405)$ is regarded as the first excited state of orbital motion among u, d, and s quarks. On the other hand, there is a long-standing argument if it is a bound state of an anti-kaon ($\bar{K}$) and a nucleon (N) since its mass is located just below the sum of $\bar{K}$ and N masses. Recently, a broad peak is observed at $\sim$100 MeV below the $\bar{K}NN$ mass threshold in the Λp invariant mass spectrum measured in the $K^-{}^3\mathrm{He} \to n\Lambda p$ reaction [1, 2]. A plausible interpretation of the peak is a $\bar{K}NN$ bound state. The properties of $\Lambda(1405)$ with respect to the $\bar{K}N$ interaction provide fundamental information to understand kaonic nuclear systems and a possible kaon condensate in ultra-dense nuclear matter, such as neutron star cores.

There exist many experimental and theoretical efforts to investigate the properties of $\Lambda(1405)$. For reference, see recent reviews [3, 4]. Based on the unitarized chiral perturbation theory in meson-baryon scattering, there are two resonance poles of Λ hyperons with the spin/parity of $1/2^-$ below the $\bar{K}N$ mass threshold, which are referred as $\Lambda(1380)$ and $\Lambda(1405)$ in the latest PDG review [5]. There seems to be a consensus on double pole structure of $\Lambda(1405)$ through intensive discussions over the last two decades. These arguments suggest that $\Lambda(1405)$ is a dynamically generated state of $\bar{K}N$. Since the $\Lambda(1405)$ resonance is located below the $\bar{K}N$ mass threshold, it has been measured in the $\pi\Sigma$ invariant mass spectra. Interpretation of line shapes of $\pi\Sigma$ invariant mass spectra at the $\Lambda(1405)$ mass region may not be straightforward in the case that the reaction mechanism to induce the $\pi\Sigma$ final state is unclear. Therefore, experimental data to extract the $\bar{K}N$ scattering amplitude at the $\Lambda(1405)$ mass region are of vital importance. This article reports our recent experimental result that the $\bar{K}N$ scattering amplitude and a resonance pole in the isospin $I = 0$ channel are successfully deduced below the $\bar{K}N$ mass threshold, based on reference [6].

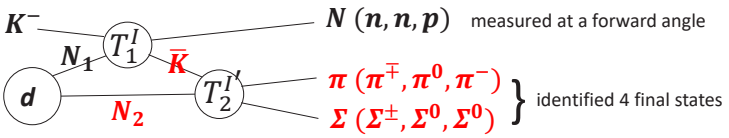

Figure 1. Reaction diagram of two-step process in the $K^-d \to N\pi\Sigma$ reaction. This process is dominant in the case that an energetic nucleon is knocked out at a very forward angle by the incident K^-.

2 Experiment

We measured $\pi\Sigma$ invariant mass spectra below and above the $\bar{K}N$ mass threshold in the $K^-d \to N\pi\Sigma$ reactions in order to study the $\bar{K}N$ interaction and the $\Lambda(1405)$ resonance. For this purpose, a negatively-charged kaon (K^-) beam of 1 GeV/c was irradiated on a deuterium target at the K1.8BR beam line in the J-PARC Hadron Experimental Facility. In the experiment, a nucleon knocked out from a deuteron (d) by an incident K^- was detected at a very forward angle, and four different final states of $\pi^+\Sigma^-$, $\pi^-\Sigma^+$, $\pi^0\Sigma^0$, and $\pi^-\Sigma^0$ were identified by measuring charged particles emitted around the target. The experimental setup is described in reference [6].

This reaction can be described by the two-step process; (i) $K^-N_1 \to \bar{K}N$ takes place followed by (ii) $\bar{K}N_2 \to \pi\Sigma$, as illustrated in figure 1. Here, N_1 and N_2 denote nucleons bound in the deuteron. Since the nucleon emitted at the forward angle carries away most of the collision energy in (i), the recoil $\bar{K}$ slows down. The center-of-mass energy in (ii) can be lower, even below the $\bar{K}N$ mass threshold because both of the $\bar{K}$ and N_2 are off-mass shell particles. Around the $\bar{K}N$ mass region, the recoil momentum of $\bar{K}$ is typically as low as ~250 MeV/c. Thus, one expects that the S-wave $\bar{K}N_2 \to \pi\Sigma$ scattering is dominant.

The $\pi\Sigma$ production cross sections can be described with T_1^I and $T_2^{I'}$, the scattering amplitude of the first-step and second-step two-body $K^-N_1 \to \bar{K}N$ and $\bar{K}N_2 \to \pi\Sigma$ reactions with isospin I and I', respectively, as follows;

$$\frac{d\sigma}{d\Omega}(\pi^{\pm}\Sigma^{\mp}) \propto \left| \frac{3T_1^{I=0} - T_1^{I=1}}{4\sqrt{3}} T_2^{I'=0} \mp \frac{T_1^{I=0} + T_1^{I=1}}{4\sqrt{2}} T_2^{I'=1} \right|^2, \quad (1)$$

$$\frac{d\sigma}{d\Omega}(\pi^-\Sigma^0) \propto \left| -\frac{T_1^{I=0} + T_1^{I=1}}{4} T_2^{I'=1} \right|^2, \quad (2)$$

$$\frac{d\sigma}{d\Omega}(\pi^0\Sigma^0) \propto \left| -\frac{3T_1^{I=0} - T_1^{I=1}}{4\sqrt{3}} T_2^{I'=0} \right|^2. \quad (3)$$

From these equations, one finds that an isospin relation of the cross sections among the four $\pi\Sigma$ final states is satisfied as

$$\frac{d\sigma}{d\Omega}(\pi^0\Sigma^0) = \frac{1}{2}\left[\frac{d\sigma}{d\Omega}(\pi^+\Sigma^-) + \frac{d\sigma}{d\Omega}(\pi^-\Sigma+) - \frac{d\sigma}{d\Omega}(\pi^-\Sigma^0) \right]. \quad (4)$$

3 Measured spectra and deduced $\bar{K}N$ scattering amplitude

Measured spectra are shown in figure 2. The statistical errors and total ones (including systematic errors) are shown separately as inner and outer bars in figure 2(a) and (b), while only the total errors are shown in figure 2(c). We observed different line shapes in the $\pi^{\pm}\Sigma^{\mp}$ final

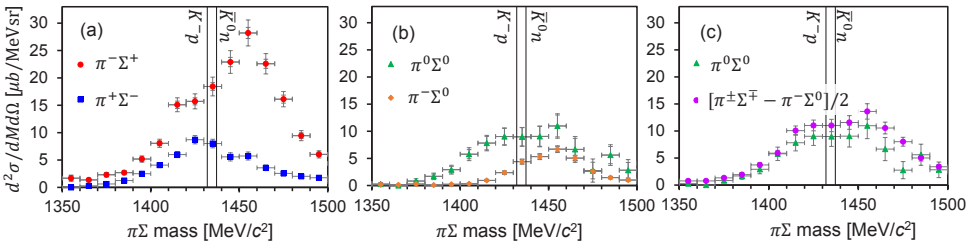

Figure 2. Measured spectra in the (a) $\pi^-\Sigma^+$ and $\pi^+\Sigma^-$, (b) $\pi^0\Sigma^0$ and $\pi^-\Sigma^0$ final states as a function of the $\pi\Sigma$ invariant mass. (c) The isospin relation in equation (4) is demonstrated.

states [figure 2(a)]. The difference is due to interference between the $I = 0$ and 1 amplitudes. In the $\pi^0\Sigma^0$ and $\pi^-\Sigma^0$ final states [figure 2(b)], only the $I = 0$ and 1 amplitudes contribute to the spectra, respectively. The strength of the $\pi^-\Sigma^0$ spectrum is smaller than that of the $\pi^0\Sigma^0$ spectrum. We find that the $I = 0$ amplitude is dominant, particularly below the $\bar{K}N$ mass threshold. We find no structure at around 1385 MeV/c^2 in the $\pi^-\Sigma^0$ spectrum, where we might expect a structure of the $\Sigma^*(1385)$ resonance. This fact supports dominance of S-wave $\pi\Sigma$ production in the present reactions since a P-wave contribution is required to excite $\Sigma^*(1385)$. The isospin relation as shown in equation (4) is demonstrated in figure 2(c).

We describe the $\pi\Sigma$ production cross section in the case of process (3) as

$$\frac{d^2\sigma}{dM_{\pi\Sigma}d\Omega_n} \approx \left|T_2^{I'}(\bar{K}N_2, \pi\Sigma)\right|^2 F_{\rm res}(M_{\pi\Sigma}), \tag{5}$$

$$F_{\rm res}(M_{\pi\Sigma}) = p_\pi^{cm} p_n^2/|(E_{K^-} + m_d)\beta_n - p_{K^-}\cos\theta_n| \int d\Omega_\pi^{cm} E_\pi E_\Sigma \times \tag{6}$$

$$\left| \int q_{N_2} T_1^I(p_{K^-}, q_{N_1}, p_n, q_{\bar{K}}, \cos\theta_{n\bar{K}}) G_0(q_{N_2}, q_{\bar{K}}) \Phi_d(q_{N_2}) d^3 q_{N_2} \right|^2, \tag{7}$$

where the $\pi\Sigma$ spectrum can be decomposed into $T_2^{I'}(\bar{K}N_2, \pi\Sigma)$ and the response function $F_{\rm res}$. Giving the scattering amplitude $T_1^I(p_{K^-}, q_{N_1}, p_n, q_{\bar{K}}, \cos\theta_{n\bar{K}})$ [8] and the deuteron wave function Φ_d [9], $F_{\rm res}$ can be calculated. Here, G_0 is the Green's function which describes the intermediate $\bar{K}$ propagation between the two vertices. A prescription to evaluate the integration of eqation (7) is described in reference [7]. For S-wave $T_2^{I'}$, we consider the $\bar{K}N$-$\pi\Sigma$ coupled channel T matrix. The diagonal and off-diagonal matrix elements can be parametrized as

$$T_2^{I'}(\bar{K}N, \bar{K}N) = \frac{A^{I'}}{1 - iA^{I'}k_2 + \frac{1}{2}A^{I'}R^{I'}k_2^2}, \tag{8}$$

$$T_2^{I'}(\bar{K}N, \pi\Sigma) = \frac{e^{i\delta^{I'}}}{\sqrt{k_1}} \frac{\sqrt{{\rm Im}A^{I'} - \frac{1}{2}|A^{I'}|^2 {\rm Im}R^{I'}k_2^2}}{1 - iA^{I'}k_2 + \frac{1}{2}A^{I'}R^{I'}k_2^2}, \tag{9}$$

where $A^{I'}$, $R^{I'}$, and $\delta^{I'}$ are the complex scattering length, complex effective range, and real phase, respectively. k_1 and k_2 are respectively the momenta of π and $\bar{K}$ in the center of mass frame. The parametrization in equation (8) is the so-called effective range expansion of the $\bar{K}N \to \bar{K}N$ scattering amplitude, where the cotangent of the phase shift is expanded to $O(k_2^2)$. Then, $T_2^{I'}(\bar{K}N, \pi\Sigma)$ is deduced from the relation of the 2×2 T-matrix, $|T_{11}|^2 + |T_{12}|^2 = {\rm Im}T_{11}$, that is obtained from the unitarity relationship of the S-matrix ($S = I + 2iT$). Here, $T_{11} = k_1 T_2^{I'}(\bar{K}N, \bar{K}N)$ and $T_{12} = \sqrt{k_1}\sqrt{k_2}T_2^{I'}(\bar{K}N, \pi\Sigma)$.

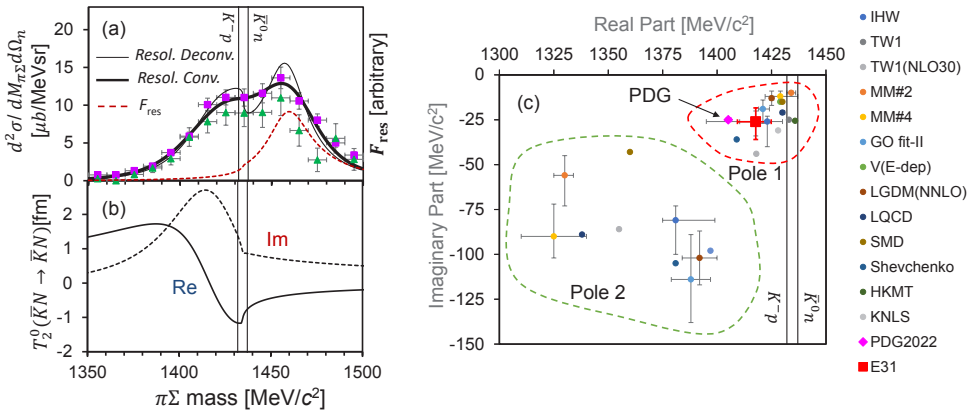

Figure 3. (a) Calculated $\pi\Sigma$ spectrum to fit the measured spectrum in the $I = 0$ channel. The solid thick and thin lines are the spectrum with and without the resolution function convoluted, respectively. The response function $F_{\rm res}$ is shown as a dashed line in arbitrary units. (b) Deduced scattering amplitude of $\bar{K}N \to \bar{K}N$ in the $I = 0$ channel. The real and imaginary parts are shown as solid and dashed lines, respectively. The vertical thin lines show the K^-p and K^0n mass thresholds. (c) The pole position deduced in the present experiment (labelled as E31) is plotted in the complex energy plane, together with the theoretical calculations and the so-called PDG value of $\Lambda(1405)$. In the legend, IHW:[10], TW1/TW1(NLO30):[11], MM#2/#4:[12], GO fit-II:[13], V(E-dep):[14], LGDM(NNLO):[15], LQCD:[16], SMD:[17], Shevchenko:[18], HKMT:[19], KNLS:[20], PDG2022:[5], E31:[6].

The values A^0 and R^0 were determined so as to reproduce the measured $\pi^0\Sigma^0$ and $(\pi^+\Sigma^- + \pi^-\Sigma^+ - \pi^-\Sigma^0)/2$ spectra, simultaneously, as shown in figure 3(a). We took the $\bar{K}N$ mass threshold at the average of K^-p and K^0n. However, we took into account the differences from the fitting results for the cases of the K^-p and K^0n mass thresholds as systematic errors. In the fitting, the experimental resolution function was convoluted with the calculated spectrum and the vertical scale is arbitrarily adjusted. The line shapes of the $\pi\Sigma$ mass spectra above the $\bar{K}N$ mass threshold are characterized by $F_{\rm res}$, the distribution of which reflects the Fermi motion of a nucleon in the deuteron, as shown by the dashed line in figure. 3(a). We obtained $A^0 = [-1.12 \pm 0.11({\rm fit})^{+0.10}_{-0.07}({\rm syst.})] + [0.84 \pm 0.12({\rm fit})^{+0.08}_{-0.07}({\rm syst.})]i$ fm, $R^0 = [-0.18 \pm 0.31({\rm fit})^{+0.08}_{-0.06}({\rm syst.})] + [-0.40 \pm 0.13({\rm fit}) \pm 0.09({\rm syst.})]i$ fm, where the fitting errors are indicated as "(fit)". As mentioned above, the differences of the different $\bar{K}N$ mass threshold were taken into account as systematic errors indicated as "(syst.)". The reduced chi-square was 1.76 with 24 degrees of freedom. Figure 3(b) plots the deduced real and imaginary part of $T_2^0(\bar{K}N, \bar{K}N)$ separately as a function of the $\pi\Sigma$ mass, from which we find a resonance pole at $1417.7^{+6.0}_{-7.4}({\rm fit})^{+1.1}_{-1.0}({\rm syst.}) + [-26.1^{+6.0}_{-7.9}({\rm fit})^{+1.7}_{-2.0}({\rm syst.})]i$ MeV/c^2. The errors are estimated by fluctuations of the pole position due to the errors for the best fit values of A^0 and R^0. The pole position deduced in the present experiment (labelled as E31) is plotted in the complex energy plane, together with the theoretical calculations [10–20] and the so-called PDG value of $\Lambda(1405)$ [5], as shown in figure 3. The theoretical analyses figure out so-called double pole structure indicated as Pole 1 and 2. The present result is located in the Pole 1 region, which is coupled to the $\bar{K}N$ channel. The real part of the deduced pole is closer to the K^-p mass threshold than the so-called PDG value of 1405.1 MeV/c^2. The deduced pole is consistent with that reported in reference [21], in which one single pole of $\Lambda(1405)$ is de-

duced by fitting the data of γ and K^- induced reactions on proton and the kaonic hydrogen atom.

4 Concluding remarks

- We measured the $\pi\Sigma$ mass spectra in the $K^-d \to N\pi\Sigma$ reactions, measuring a knocked-out N at ∼0 degree.
  - The reactions are well described with the two-step reaction process: $K^-N_1 \to N\bar{K}$ followed by $\bar{K}N_2 \to \pi\Sigma$.
  - The S-wave $\bar{K}N_2 \to \pi\Sigma$ scattering is dominant as no $\Sigma^*(1385)$ is observed in the $\pi^-\Sigma^0$ spectrum, suggesting that P-wave contribution is negligible.
  - The measured spectra safisfy the isospin relation of equation (4).
- The S-wave $\bar{K}N$ scattering amplitude (I=0) in the framework of $\bar{K}N$-$\pi\Sigma$ coupled channel was obtained so as to reproduce the measured $\pi\Sigma$ spectra below and above the $\bar{K}N$ mass threshold.
- We found a resonance pole at $1417.7 - 26.1i$ [MeV], which seems consistent to that of the so-called higher pole of $\Lambda(1405)$ suggested by the unitarized chiral perturbation theory.

References

[1] S. Ajimura *et al*., Phys. Lett. B **789**, 620(2019).
[2] T. Yamaga *et al*., Phys. Rev. C **102**, 044002(2020).
[3] M. Mai, Eur. Phys. J. Spec. Top. **230**, 1593(2021).
[4] T. Hyodo, M. Niiyama, Prog. Part. Nucl. Phys. **120**, 103868(2021).
[5] R. L. Workman *et al*. (Particle Data Group), Review of Particle Physics, Prog. Theor. Exp. Phys. **2022**, 083C01(2022).
[6] S. Aikawa *et al*., Phys. Lett. B **837**, 137637(2023).
[7] K. Miyagawa and J. Haidenbauer, Phys. Rev. C **85**, 065201(2012).
[8] G. P. Gopal *et al*., Nucl. Phys. B **119**, 362(1977).
[9] R. Machleidt, Phys. Rev. C **63**, 024001(2001).
[10] Y. Ikeda, T. Hyodo, W. Weise, Nucl. Phys. A **881**, 98(2012).
[11] A. Cieply, J. Smejkal, Nucl. Phys. A **881**, 115(2012).
[12] M. Mai and U.-G. Meißner, Eur. Phys. J. A **51**, 30(2015).
[13] Z.-H. Guo and J. A. Oller, Phys. Rev. C **87**, 035202(2013).
[14] T. Ohnishi, Y. Ikeda, T. Hyodo, and W. Weise, Phys. Rev. C **93**, 025207(2016).
[15] J.-X. Lu, L.-S. Geng, M. Döring, and M. Mai, Phys. Rev. Lett. **130**, 071902(2023).
[16] Z. W. Liu, M. M. Hall, D. B. Leinweber, A. W. Thomas, and J. J. Wu, Phys. Rev. D **95**, 014506(2017).
[17] D. Sadasivan, M. Mai, M. Döring, Phys. Lett. B **789**, 329(2019).
[18] N. V. Shevchenko, Phys. Rev. C **85**, 034001(2012).
[19] J. Haidenbauer, G. Krein, U.-G. Meißner, and L. Tolos, Eur. Phys. J. A **47**, 18(2011).
[20] H. Kamano, S. X. Nakamura, T.-S. H. Lee, T. Sato, Phys. Rev. C **92**, 025205(2015).
[21] A.V. Anisovich, A. V. Sarantsev, V. A. Nikonov, V. Burkert, R. A. Schumacher, U. Thoma, and E. Klempt, Eur. Phys. J. A **56**, 139(2020).